# Numerical Study of Impulsive Wave Overtopping at Rigid Hydraulic Structures Using Incompressible Smoothed Particle Hydrodynamics Model

Rasoul Memarzadeh[1]

1. Department of Civil Engineering, Faculty of Engineering, Vali-e-Asr University of Rafsanjan, Iran, P.O. Box 518.

***Corresponding Author:**
Rasoul Memarzadeh,

**Email:** r.memarzadeh@vru.ac.ir
**Received:** 2025.03.22
**Accepted:** 2025.07.21
**J. Hydraul. Struct., 2025; 12(2):51-73**
**DOI: 10.22055/jhs.2025.48919.1345**

## ABSTRACT

Understanding the behavior of wave overtopping at hydraulic structures is critical for ensuring the stability and longevity of dams and coastal defenses. This study presents a validated Incompressible Smoothed Particle Hydrodynamics – Large Eddy Simulation (ISPH–LES) model for accurately simulating solitary wave overtopping events. The ISPH–LES model integrates advanced improvements, including a newly developed solid boundary treatment that enhances numerical stability and fidelity near rigid walls. Given the highly turbulent nature of overtopping flows, the integration of LES into the SPH framework enables detailed resolution of vortex structures and energy dissipation mechanisms. The model was validated against experimental data from nine overtopping scenarios, with predictions of key hydrodynamic parameters—maximum overtopping depth, overtopping volume, and wave overtopping duration—yielding average errors of 9.5%, 15%, and 5.9%, respectively. Temporal pressure distributions over 27 time frames were analyzed to illustrate the model's ability to capture impact, peak, and dissipation phases of overtopping. The results indicate that the ISPH–LES model performs exceptionally well in high-energy overtopping events, while suggesting potential refinements in scenarios with smaller overtopping volumes. These findings underscore the model's practical utility for designing hydraulic structures in regions prone to extreme wave conditions, offering critical insights into optimizing structural resilience under a wide range of overtopping scenarios

## KEYWORDS

Numerical study, ISPH – LES model, Modified wall boundary condition, Solitary impulse wave, Rigid hydraulic structures, Wave overtopping.

## 1. Introduction

Dams and coastal defense structures, whether human-made or natural, are designed to suppress floods and protect urban, industrial, or agricultural areas. The weakness in the performance of these structures can lead to downstream flooding. One of the main concerns in designing dams and breakwaters is their stability. One of the important issues that can cause the hydraulic structures to be unstable is the overtopping caused by different waves created on the coats or dam's reservoir. The waves in dam reservoirs are caused by a variety of factors, including wind and landslides. On the coastal areas, waves are also caused by factors such as submarine earthquakes, tides and marine storms.

The purpose of the present study is to investigate the overtopping of shock waves at hydraulic structures such as waves from materials collapsing in dams or tsunami waves from marine breakwater.

Turbulence modeling plays a pivotal role in the accurate simulation of complex hydraulic flows associated with hydraulic structures such as gates, spillways, and overtopping scenarios. These flows are characterized by high-energy transitions, rapid depth changes, and multi-scale vortical structures that demand robust and high-fidelity numerical modeling approaches. The flow examined in this study—consisting of a high-speed, high-energy solitary wave impacting a rigid structure—undergoes significant changes in depth, velocity, and turbulence, making it inherently complex and highly unsteady. Similar to the turbulent flow fields passing through gates or spillways, this type of flow involves intricate vortex formations and energy dissipation patterns. Capturing these turbulent structures with precision is essential to improving the predictive capability and reliability of hydrodynamic simulations. Previous studies have demonstrated the necessity of using advanced turbulence-resolving models in such applications. For example, Kheybar et al. [1] studied the hydraulic performance of pivot side weirs with sills; Tahmasbipour et al. [2] examined T-jump stabilization mechanisms using water jets and corrugated beds; and Taheri Talavari et al. [3] conducted a numerical analysis of flow behavior through multiple elliptic Lopac gates. Similarly, advanced CFD approaches were employed by Ahadiyan et al. [4] to optimize flexible gate operations in intake systems, and Shahabi et al. [5] revealed turbulence patterns in V-shaped fishways. Furthermore, turbulent interactions of counter-flow jets [6], elliptical Lopac gate flows [7], sudden canal contractions [8], energy losses in stepped spillways [9], and the effects of vortex breakers in morning glory spillways [10] have all underscored the importance of using high-fidelity turbulence models in hydraulic simulations.

In this context, solitary waves offer a valuable and widely accepted benchmark for evaluating the performance of turbulence-resolving hydrodynamic models of overtopping problems. Although solitary waves are idealized and not fully representative of real-world storm waves or tsunamis, they effectively replicate the key characteristics of impulsive wave events - namely, rapid onset, high velocity, and concentrated energy. These attributes make solitary waves particularly suitable for investigating wave-structure interactions under extreme conditions such as landslide-induced waves or tsunami impacts. Their use in numerical simulations allows for controlled, repeatable testing of model performance in capturing complex free surface dynamics, turbulent vortex development, and energy dissipation processes critical to structural safety assessments.

Due to the importance of wave overtopping from coastal structures and dams, many researchers have investigated it from different perspectives. EurOtop [11] have studied the different characteristics of the oscillatory wave overtopping from coastal defense structures, and they presented details of this phenomenon in a manual design. In Chapter 5 of this manual, the relationships of oscillatory wave overtopping with different return periods for different configurations of breakwater were presented. In this chapter, they present the relationships for calculating discharge and flow volume due to oscillatory wave overtopping with specified return periods by considering effect of various parameters such as roughness, oblique waves, wave walls for simple and composite coastal dikes [11]. Despite extensive study of oscillatory wave overtopping at sea defense structures, the overtopping of impulsive waves has been studied less [11]. Examples of the studies in this area are Özhan and Yalçıner [12], Müller [13], Jervis and Peregrine [14], Stansby [15], Xiao et al.

[16], Heller et al. [17], Kobel et al. [18] and chi et al. [14]. In these studies, different equations have been proposed to predict the volume of flow overtopping.

The study method for presenting the equations of wave overtopping in the mentioned studies was physical modeling. Analytical, experimental and numerical methods can be used to calculate wave overtopping characteristics from structures including flow volume. An important advantage of validated numerical models for the study of wave overtopping from hydraulic structures is their non-limitation for structures with different designs [11]. The available numerical models for studying the overtopping are nonlinear shallow water equations models and Navier-Stokes equations models [11]. Navier-Stokes equations models are generally based on one of two categories techniques including Volume of Fluid (VOF) method [20] and Smoothed Particle Hydrodynamics (SPH) method [21]. SKYLLA model based on VOF method is one of the business models available for studying the overtopping at coastal structures [22]. This model can be easily applied to model the overtopping caused by regular waves at breakwaters.

In the present paper, a two-dimensional vertical (2DV) model based on Incompressible Smoothed Particle Hydrodynamics (ISPH) method with sub-particle scale – large eddy simulation (SPS - LES) closure model is developed to study the impulsive wave overtopping at hydraulic structures. The SPH method is an integral interpolation-based method in which the computational domain is expressed by particles containing physical properties including mass and density [23]. Details about the SPH method can be found in the previous research e.g. Monaghan [21]. The SPH method has two different approaches for calculating pressure of particles; weakly compressible perspective (WCSPH) and incompressible perspective (ISPH) [24]. Since its introduction by Monaghan [21], this method has rapidly evolved, and it has been used successfully to study various hydraulic problems (e.g. [25-32]).

In the case of impulsive wave overtopping at hydraulic structures, despite the proven power of the SPH method in simulating high varied free surface flows, this method has not been used to study the details of this phenomenon with different conditions. However, the solitary wave overtopping problem is one of the main benchmarks for evaluation of the accuracy of developed models by SPH method (e.g. Akbari [33]). In one study related to mesh-less Lagrangian methods, Luo et al. [34] developed a 2DV CPM-based hydrodynamic model for studies of some properties of solitary wave impinging on and overtopping a seawall. In their study, they demonstrated the effectiveness of the CPM hydrodynamic model for simulating solitary wave impact on a seawall. Then, using the numerical model, a parametric study was carried out to investigate the effect of transverse cross-section geometry on wave overtopping properties. Therefore, in the present study the ISPH - LES hydrodynamics model has been utilized to investigate the solitary wave overtopping at rigid hydraulic structures.

Large Eddy Simulation (LES) is a high-fidelity turbulence modeling approach widely employed in fluid dynamics to resolve the behavior of large-scale turbulent structures while modeling the effects of smaller, subgrid-scale (SGS) motions. Unlike Reynolds-Averaged Navier–Stokes (RANS) models, which average all turbulent fluctuations, LES resolves the larger, energy-containing eddies directly, capturing transient and spatially-evolving phenomena more accurately. This makes LES especially suitable for simulating highly unsteady and vortical flows, such as those found in wave breaking, overtopping, or jet impingement in hydraulic engineering. In the context of mesh-free numerical methods like Smoothed Particle Hydrodynamics (SPH), LES offers a promising pathway for enhancing turbulence representation without the excessive computational cost of Direct

Numerical Simulation (DNS) [24]. The ability of LES to simulate vortex shedding, turbulence dissipation, and transitional flow regimes makes it a critical tool for high-resolution hydrodynamic studies involving free-surface and multiphase interactions.

This study introduces a two-dimensional Incompressible Smoothed Particle Hydrodynamics – Large Eddy Simulation (ISPH–LES) model developed for detailed simulation of solitary wave overtopping at rigid hydraulic structures. Recognizing the complex and highly dynamic nature of such flows—particularly near solid boundaries—the model incorporates advanced modifications, including an improved wall-boundary pressure treatment. This enhancement effectively prevents the penetration of flow particles into rigid boundaries and ensures higher numerical stability and fidelity in simulating wave-structure interactions. To comprehensively validate the model's performance, the simulation results were compared with experimental data from Kobel et al. [18], focusing on critical hydrodynamic parameters such as wave profile evolution, overtopping depth, overtopping volume, and overtopping duration. Given the critical importance of accurate overtopping prediction for the safety of hydraulic infrastructures, the integration of LES turbulence modeling with SPH offers a powerful approach to capturing the intricate turbulent structures and transient behaviors inherent to high-energy wave impacts. By addressing existing limitations in resolving pressure and flow characteristics during impulsive wave events, this research presents a robust numerical framework that can significantly enhance the design and safety assessments of dams, seawalls, and other coastal defense systems exposed to extreme wave conditions.

## 2. Methodology

### 2.1. Governing equations

The present ISPH–LES model solves the Navier-Stokes equations as presented below:

$$\frac{D\rho}{Dt} + \rho(\nabla \cdot \bar{u}) = 0 \quad (1)$$

$$\frac{D\bar{u}}{Dt} = -\frac{1}{\rho}\nabla P + \nu(\nabla^2 \bar{u}) + g + \frac{1}{\rho}\nabla.\vec{\tau} \quad (2)$$

Where $\rho$ and $\nu$ are density and kinematic viscosity of flow, $\bar{u}$ is velocity of flow, $P$ is pressure of flow, $\boldsymbol{g}$ is gravity force, $t$ is time, and $\vec{\tau}$ is the SPS stress tensor. The SPS stress tensor is modeled using the Boussinesq eddy viscosity assumption [23]:

$$\frac{\tau_{ij}}{\rho} = 2\nu_t \bar{E}_{ij} - \frac{2}{3}k\delta_{ij} \quad (3)$$

Where $\nu_t$ is the kinematic eddy viscosity, $\bar{E}_{ij}$ is the strain tensor, $k$ is the turbulence kinetic energy. The eddy viscosity is calculated using the standard Smagorinsky model as follows:

$$\nu_t = (C_s dr)^2 II_{\bar{E}} \quad (4)$$

In which $C_s$ is the Smagorinsky constant equal to 0.15, $dr$ is particle spacing indicating the characteristic length scale of the small eddies and $II_{\bar{E}}$ is second invariant of the filtered-field deformation tensor. The $k$ incorporated in the pressure term by defining the following equation [23]:

$$P_E = P + (\frac{2}{3})\rho k \quad (5)$$

Since in physics, $k$is much smaller than $P$, so $P$ can be used instead of $P_E$ [35]. Finally, by putting the terms of equation 3 in equation 2, the final momentum equation will be expressed as:

$$\frac{D\bar{u}}{Dt} = -\frac{1}{\rho}\nabla P + \nu_e(\nabla^2 \bar{u}) + g \quad (6)$$

Where $\nu_e$ is equal to $\nu + \nu_t$.

### 2.2. Two-step solution scheme

Solving the governing equations using the SPH method is performed with two approaches including weakly compressible

and incompressible methods. In the weakly compressible approach, which is used in standard SPH method, the pressure is calculated using the state equation based on particle density. However, in the incompressible approach, the pressure is calculated implicitly by applying the incompressible conditions. The model developed in this study is based on the incompressible approach. The present ISPH – LES model follows the following steps to calculate the results:

Firstly, the second principal invariant of the tensor of shear strain rate is calculated, and the eddy viscosity of particles is calculated using equation (4).

Secondly, which is known as the predictor step, the temporary position and velocity of particles ($u^*$ and $r^*$) are computed by neglecting the pressure gradient term:

$$u^* = u^t + \Delta t(\nu_e \nabla^2 . u + g)^t \quad (7)$$

$$r^* = r^t + \Delta t . u^* \quad (8)$$

The discrete form of the Laplacian of the viscosity term in equation (7) using the SPH method formulation is the following equation [35]:

$$(\nu_e \nabla^2 . u)_i \approx \sum_j \frac{2m_j((\nu_e)_i + (\nu_e)_j) r_{ij} . \nabla_i \hat{W}_{ij}}{(\rho_i + \rho_j)(|r_{ij}|^2 + \lambda^2)} (u_i . u_j) \quad (9)$$

Where $\hat{W}$ is the interpolation kernel function, $\boldsymbol{r}$ is position vector, $r_{ij} = r_i - r_j$ and $\lambda$ is a constant small number.

Thirdly, which is known as the corrector step, the pressure Poisson equation is solved to calculate the pressure of particles:

$$\nabla . (\frac{1}{\rho_*} \nabla P_{t+1}) = \frac{\rho_0 - \rho_*}{\rho_0 \Delta t^2} \quad (10)$$

Where $\rho_0$ is the density of particles at the current time step, and $\rho_*$ is the intermediate density of particles. Employing the relevant SPH formulation to the left-hand side of equation (10), a linear equation system can be obtained [23]:

$$\nabla . (\frac{1}{\rho} \nabla P)_i \approx \sum_j m_j \frac{8}{(\rho_i + \rho_j)^2} \frac{P_{ij} \mathbf{r}_{ij} . \nabla_i W_{ij}}{|\mathbf{r}_{ij}|^2 + \lambda^2} \quad (11)$$

Fourthly, the new velocities of particles are computed by the equations (12) and (13):

$$u^{t+1}{}_{=u^*} + \Delta t(-\frac{1}{\rho^*} \nabla P^{t+1}) \quad (12)$$

$$r^{t+1} = r^t + \frac{u^{t+1} + u^t}{2} \Delta t \quad (13)$$

## 2.3. Improved solid boundary conditions

In the present model, the solid boundary condition is implemented by using fixed particles as wall particles and placing multiple rows of dummy particles outside the wall particles. The Newman boundary condition is established by equating the pressure of wall particles with dummy particles perpendicular to them. In this method, the governing equations for these particles are solved like the flow particles. As the flow particles approach the wall particles, the pressure in them will be calculated so that the flow particles will not penetrate the wall. This solid boundary condition has been widely used in previous researches, and it has presented satisfactory results e.g. Shao and Lo [36], Shao [37], Memarzadeh and Hejazi [26], and Akbari [33]. However, when the velocities of particles are high near the wall particles, some of them will penetrate the wall. For this purpose, the additional pressure term, called molecular force, is applied to the calculated pressure for the wall particles. This term was first introduced by Monaghan [21] to simulate the wall particles in the standard SPH method. The essence of this term is that if the distance between the wall particle and its adjacent fluid particles is reduced to a certain distance that allows water particles to penetrate the wall, the following equation is added to the wall particle pressure:

$$f(r) = \frac{d_0}{r}((\frac{r_0}{r})^4 - (\frac{r_0}{r})^2) \quad (14)$$

Where $r$ is the distance between the wall particle and the water particles in its neighborhood, $d_0$ is a fixed number equal to 5 and $r_0$ is $0.9 \times dr$. By applying this additional term, the flow particle motion modeling adjacent to wall particles has been more accurately performed.

## 2.4. Free surface boundary conditions

In this study, the free surface boundary condition was determined using the particle density criterion. Specifically, particles with a density between 0.9 and 0.99 times the reference water density were identified as free surface particles. A zero-pressure condition was then applied to these particles to simulate atmospheric exposure. Additionally, to ensure the stability and accuracy of pressure calculations near the free surface, a pressure gradient symmetry condition was imposed. This approach assumes that the pressure distribution across the free surface behaves symmetrically, thereby avoiding artificial pressure spikes and ensuring a smooth transition in the pressure field.

## 2.5. Description of the problem used to evaluate the ISPH–LES hydrodynamic model

Validating the ISPH–LES hydrodynamic model against the experimental results of Kobel et al. [18] represents a crucial step toward ensuring its accuracy in simulating complex hydrodynamic phenomena like solitary wave overtopping at rigid hydraulic structures. The experimental data gathered at ETH Zurich provides a robust framework for comparison, with precise measurements of key overtopping parameters under carefully controlled conditions.

Kobel et al. [18] experimentally studied solitary wave overtopping at a rigid dam in various scenarios at ETH University, Zurich. Their experiments were conducted in a laboratory flume measuring 11 m in length and 0.5 m in width. The solitary wave in this flume was generated by a piston type wave maker located 4.85 meters from the dam. The dam structure and flume are made of PVC and glass, respectively. The height of the dam ($HD$) is considered constant at 30 cm. In their study, three parameters including the wave overtopping volume ($V$), maximum wave overtopping depth ($d_{max}$) and wave overtopping duration ($t_0$) have been studied. In mentioned study, the effect of water depth behind dam ($h$), wave height ($a$), dam angle in reservoir ($\beta$) and dam crest width ($b_k$) were investigated as influential parameters on hydrodynamics of solitary wave overtopping. The schematic illustration of the geometry of the problem is shown in Figure 1. In the study of Kobel et al. [18] 75 tests have been performed. From these tests, nine tests have been selected for the validation of the present ISPH – LES model as described in Table 1. The intended tests are selected so that all the important parameters in the solitary wave overtopping can be seen. In cases of 1, 2 and 3, the effect of solitary wave height, in cases of 4 and 5, the effect of water depth, in cases of 6 and 7, the effect of dam angle in reservoir, and finally in cases of 8 and 9, the effect of dam crest width in the overtopping of solitary wave from the rigid structures are numerically studied.

The free surface profiles and the initial velocity of the solitary wave based on the analytical solution of the Boussinesq equation are applied as follows [38]:

$$\eta(x,t) = a\ sec\, h^2\ [\sqrt{\frac{3a}{4h^3}}\ (x - ct)\ ] \quad (15)$$

$$u = \eta\sqrt{\frac{g}{d}} \quad (16)$$

Where $\eta$ is water surface elevation, $c = \sqrt{g(d+a)}$ is wave celerity and $t$ is time of propagation. In the numerical modeling, the initial diameter of the particles was considered to be 0.0125 m after performing convergence analysis and ensuring the best results. It is worth noting that the functional

form of Equation (15), which describes the free surface elevation of a solitary wave, bears a close resemblance to the Gaussian distribution. This similarity is not coincidental—it reflects the localized, symmetric nature of solitary waves. Physically, the shape results from a balance between nonlinear steepening and dispersive spreading, yielding a waveform with a smooth crest and exponentially decaying tails. While not derived from statistical considerations like the Gaussian distribution, the mathematical structure of solitary wave solutions often appears similar due to these shared characteristics of symmetry and concentration. This similarity enhances their suitability for use in numerical and analytical modeling, as they exhibit predictable, well-defined profiles that lend themselves to validation and calibration tasks.

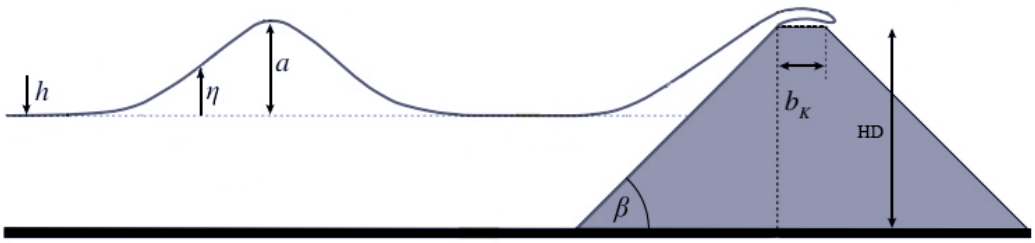



**Figure 1. Schematic diagram of the model used to evaluate the ISPH–LES model.**

**Table 1. Parameters of solitary wave overtopping at rigid dams.**

| Case number | $h\ (m)$ | $a\ (m)$ | $\varepsilon = a/h$ | $\beta$ (deg) | $b_k\ (cm)$ |
|---|---|---|---|---|---|
| 1 | 0.25 | 0.175 | 0.7 | 90 | 2 |
| 2 | 0.25 | 0.125 | 0.5 | 90 | 2 |
| 3 | 0.25 | 0.075 | 0.3 | 90 | 2 |
| 4 | 0.2 | 0.14 | 0.7 | 90 | 2 |
| 5 | 0.3 | 0.21 | 0.7 | 90 | 2 |
| 6 | 0.2 | 0.14 | 0.7 | 18.4 | 2 |
| 7 | 0.2 | 0.14 | 0.7 | 45 | 2 |
| 8 | 0.25 | 0.125 | 0.5 | 90 | 6 |
| 9 | 0.25 | 0.125 | 0.5 | 90 | 16 |

## 3. Results and discussion

### 3.1. Qualitative Comparison of Free Surface Profiles

Figure 2 provides a visual comparison of the free surface profiles of the solitary wave as it overtops the rigid dam, as predicted by the ISPH–LES model, compared with the experimental data from Kobel et al. [18]. This qualitative analysis is essential for assessing the model's ability to replicate the key physical phenomena observed during wave overtopping, including the evolution of the wave crest, the overtopping flow, and the dissipation of energy after overtopping.

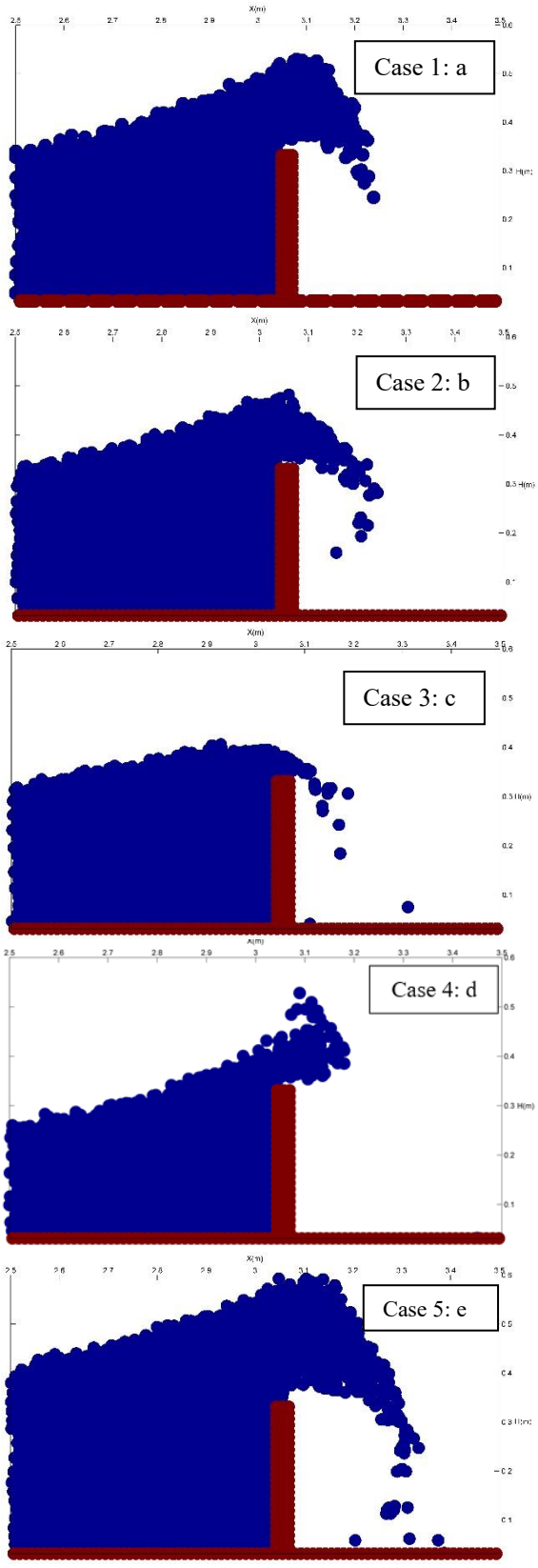
The ISPH–LES model demonstrates a high degree of agreement with the experimental data across all nine cases, capturing the nuances of wave-structure interaction. The free surface profiles at various stages of the overtopping event—particularly during the critical phases of maximum wave cresting and overtopping—are closely matched with experimental observations. Accurately simulating these stages is crucial, as they represent the moments of peak force exerted on the structure, which directly impacts its structural integrity.

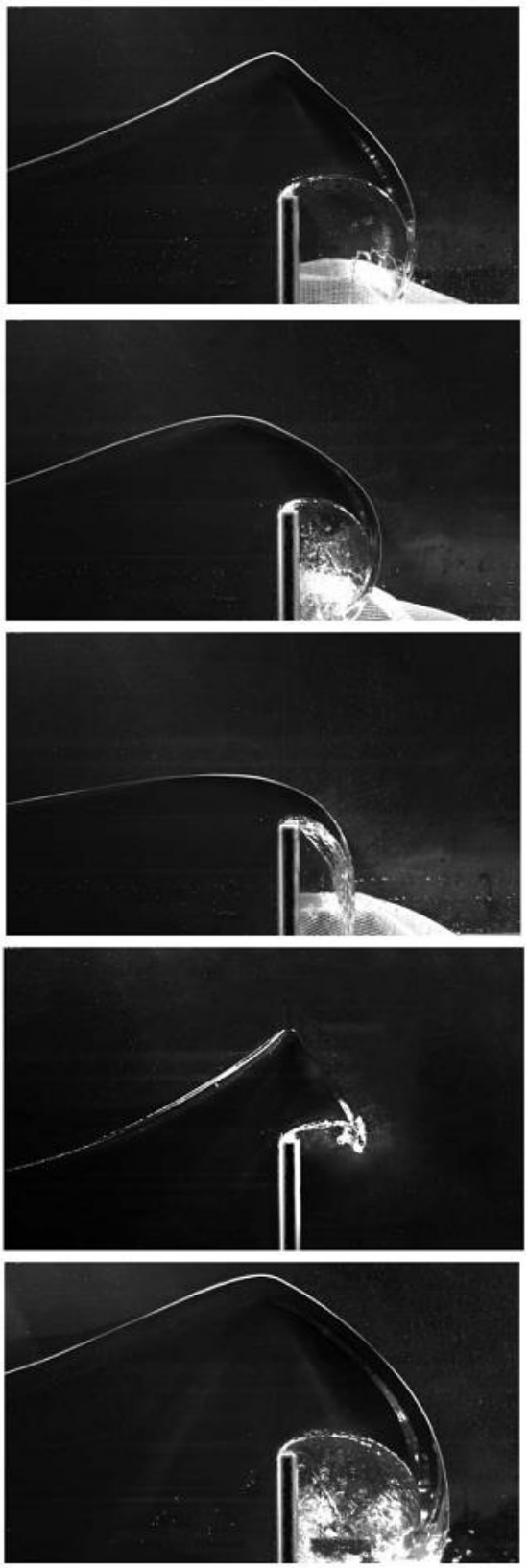
Figures 2a–2c show that as the height of the solitary wave decreases, the volume of the overtopping flow correspondingly decreases. This trend is not only consistent with the experimental data but also aligns with fundamental hydrodynamic principles, where smaller waves carry less energy and momentum, resulting in lower overtopping volumes. The ISPH model successfully captures this behavior, demonstrating its sensitivity to wave height variations—a critical factor for simulating wave forces on structures subjected to different wave conditions.

In Figures 2d and 2e, the effect of varying water depth behind the dam is clearly depicted. As expected, deeper water results in higher overtopping volumes and greater overtopping depths. This behavior is accurately modeled by the ISPH–LES model, showing that it is capable of simulating the influence of reservoir depth on overtopping dynamics. This is particularly important for hydraulic structures in environments where water levels fluctuate due to tides, seasonal changes, or other environmental factors.

Figures 1f and 1g show the influence of sloping the dam. The introduction of a slope reduces the height of the overtopping wave as it dissipates more energy upon impact with the angled surface. The ISPH–LES model closely mirrors this experimental result, further proving its ability to simulate how structural design modifications—such as changing the angle of the dam—affect overtopping behavior. This finding is valuable for designing dams and coastal defenses, as slope modifications can be used to mitigate the intensity of overtopping forces.

Finally, Figures 2h and 2i, which explore the effects of varying dam crest width, reveal that the ISPH–LES model performs well in simulating wave overtopping over different structural geometries. Interestingly, the results show that crest width has a relatively minor impact on the overall overtopping flow, a conclusion that is supported by both the model and the experimental data. This indicates that other factors, such as wave height and water depth, play more significant roles in determining overtopping behavior.


Case 1: a
Case 2: b
Case 3: c
Case 4: d
Case 5: e



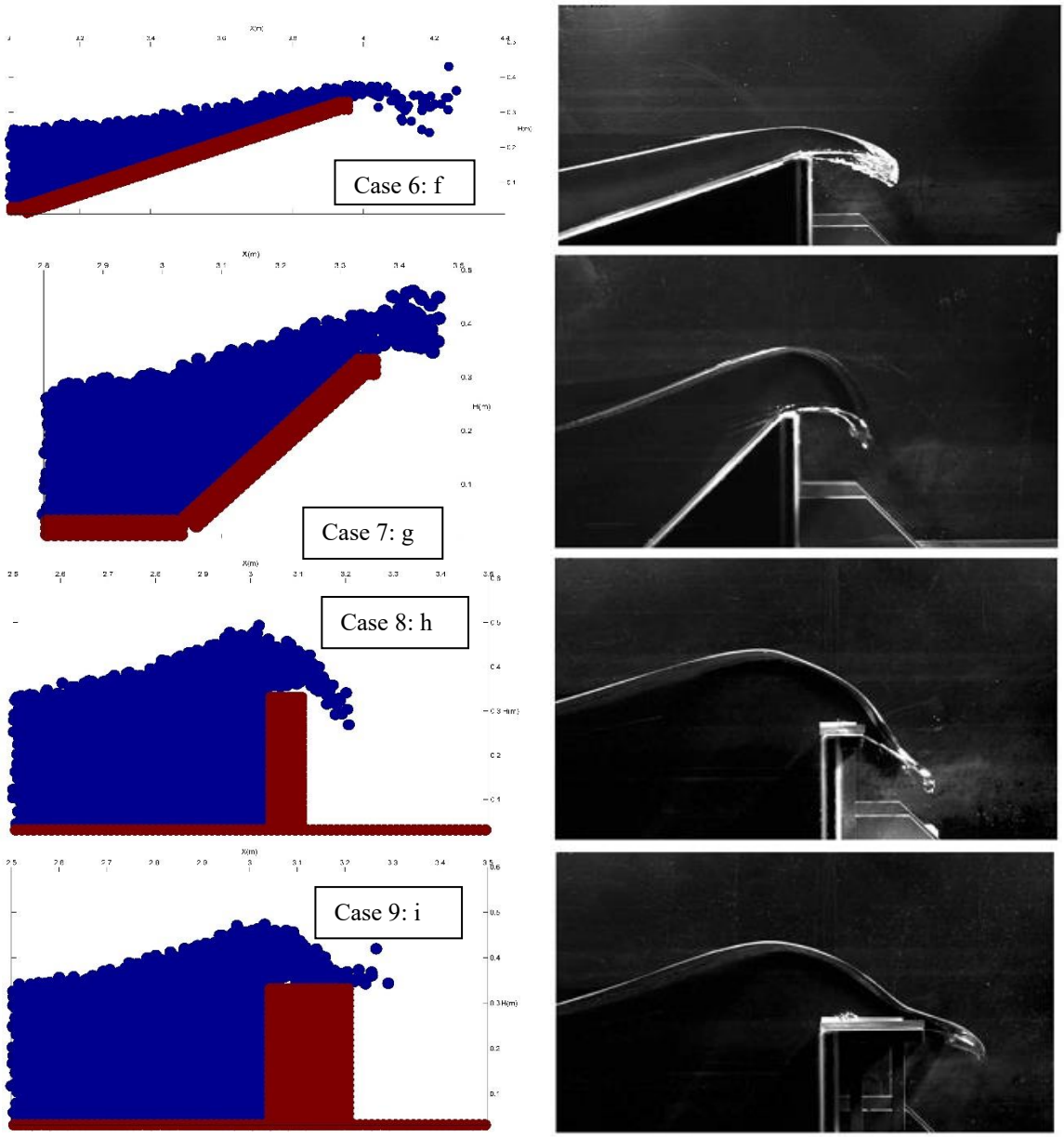



**Figure 2. Qualitative comparison of free surface profiles in the present ISPH-LES numerical model and experimental data of Kobel et al. [18] during solitary wave overtopping of the rigid structure. The horizontal and vertical axes are both meters (m).**

### 3.2. Quantitative Comparison: Maximum Overtopping Depth, Overtopping Volume, and Duration

In addition to the qualitative comparison, Table 2 presents a detailed quantitative analysis of the ISPH model's performance by comparing it with experimental data for maximum overtopping depth, overtopping volume, and wave overtopping duration. This quantitative validation is crucial for assessing the model's precision and identifying areas where further refinement may be necessary.

#### Maximum Overtopping Depth

The ISPH model shows strong performance in estimating the maximum overtopping depth, with an average error of 9.5% across all scenarios. This parameter directly reflects the peak hydraulic load exerted by incoming waves, which is critical for the design of coastal defenses

and flood protection structures. In this context, the overtopping depth serves not only as an indicator of wave intensity but also as a proxy for estimating the vertical pressure gradient and the required freeboard height in design calculations.

Case 5, which involved the most intense overtopping event, exhibited the lowest error (3.6%), corresponding to a high wave energy condition. This accuracy under extreme loading highlights the robustness of the ISPH–LES approach in capturing nonlinear wave deformation, energy transfer, and momentum flux during solitary wave impact. Such precise prediction is particularly useful for evaluating structural vulnerability under rare but destructive wave events, including those induced by landslides or tsunamis.

In contrast, Cases 6 and 7, which featured reduced wave heights and overtopping volumes, presented slightly higher errors (14.3% and 16.7%). These discrepancies may result from amplified sensitivity in small-scale flows where viscous effects, turbulence dissipation, and local flow separations play a relatively larger role. From a hydrodynamic perspective, the model still captures the trend of decreasing overtopping depth with lower wave energy but highlights the need for resolution improvement or turbulence modeling refinement in low-energy regimes.

Importantly, the ISPH model allows for dynamic tracking of free surface evolution and pressure gradients over the structure.

## Overtopping Volume

Overtopping volume is a more complex parameter due to the dynamic and transient nature of the flow during wave overtopping. The ISPH model achieved an average error of 15% in predicting overtopping volume, indicating that it performs reasonably well in capturing the flow behavior during overtopping events.

Cases 1, 8, and 9, which represent moderate to large overtopping volumes, exhibited relatively low errors (9.1% to 10.5%), demonstrating the model's strong ability to simulate overtopping in cases where wave height and flow are substantial. The alignment between the numerical and experimental results in these cases validates the model’s accuracy for predicting flow volumes under higher-energy conditions.

Cases 6 and 7, with the smallest overtopping volumes, showed the highest errors (20.00% and 22.2%, respectively). This suggests that the model's sensitivity to smaller wave volumes introduces some limitations, particularly in cases where the overtopping flow is minimal. These discrepancies highlight the need for further refinement of the ISPH model in low-volume overtopping scenarios. Potential improvements could include enhanced resolution in the particle dynamics or better handling of flow separation effects, which tend to be more pronounced in smaller overtopping events.

## Wave Overtopping Duration

The ISPH model excels in predicting wave overtopping duration, with an average error of only 5.86%. Accurate prediction of overtopping duration is crucial for understanding the long-term exposure of structures to wave forces, which has significant implications for material fatigue and structural longevity.

Cases 8 and 9, which featured longer overtopping durations, had the lowest errors (1.2%), highlighting the model’s precision in simulating sustained overtopping events. The ability to accurately capture the duration of overtopping is essential for assessing the cumulative impact of wave forces over time, particularly in environments where repeated overtopping events are expected.

Even in Case 6, where the error was highest at 10.1%, the ISPH model’s prediction remained within acceptable limits. This consistency across a range of overtopping durations reinforces the model’s reliability for simulating both short, high-intensity overtopping events and longer, more gradual flows.

**Table 2. Comparison of ISPH-LES Model Results and Experimental Data of Kobel et al. [8] for Maximum Overtopping Depth, Overtopping Volume, and Wave Overtopping Duration with Approximate Errors.**

| | Maximum Overtopping Depth (m) | | | Overtopping Volume (m^3/s) | | | Wave Overtopping Duration (s) | | |
|---|---|---|---|---|---|---|---|---|---|
| | ISPH Result | Experimental data | Approximate error | ISPH Result | Experimental data | Approximate error | ISPH Result | Experimental data | Approximate error |
| Case 1 | 0.20 | 0.22 | 9.1 | 0.017 | 0.019 | 10.5 | 0.81 | 0.86 | 5.8 |
| Case 2 | 0.13 | 0.14 | 7.1 | 0.010 | 0.012 | 16. 7 | 0.75 | 0.81 | 7.4 |
| Case 3 | 0.06 | 0.07 | 14.3 | 0.005 | 0.006 | 16.7 | 0.60 | 0.65 | 7.7 |
| Case 4 | 0.16 | 0.17 | 5.9 | 0.006 | 0.007 | 14.3 | 0.47 | 0.50 | 6.00 |
| Case 5 | 0.27 | 0.28 | 3.6 | 0.033 | 0.039 | 15.4 | 1.29 | 1.34 | 3.7 |
| Case 6 | 0.06 | 0.07 | 14.3 | 0.008 | 0.010 | 20.00 | 0.71 | 0.79 | 10.1 |
| Case 7 | 0.10 | 0.12 | 16.7 | 0.007 | 0.009 | 22.2 | 0.57 | 0.63 | 9.5 |
| Case 8 | 0.13 | 0.14 | 7.1 | 0.010 | 0.011 | 9.1 | 0.80 | 0.81 | 1.2 |
| Case 9 | 0.13 | 0.14 | 7.1 | 0.009 | 0.010 | 10.00 | 0.80 | 0.81 | 1.2 |
| Approximate average error | | | 9.5 % | Approximate average error | | 15 % | Approximate average error | | 5.9 % |

## 3.3. Pressure Distribution Analysis: A Detailed Investigation of Structural Impacts

The temporal and spatial pressure distributions predicted by the ISPH–LES model across 27-time frames for the nine test cases (Figures 3–11) provide valuable insights into wave-structure interaction dynamics. These results go beyond simple visualization, offering a deeper understanding of pressure wave propagation, reflection, dissipation, and the influence of structural geometries on pressure magnitudes. The ability to capture such high-resolution temporal behavior is critical for identifying vulnerable structural zones and designing cost-effective, durable hydraulic defenses.

### Initial Wave Impact Phase

In the early stages (first 5–10-time frames), the solitary wave approaches and collides with the upstream face of the rigid structure. In Cases 1 to 3 - representing variations in wave height - the pressure concentration is initially localized at the toe or base of the structure. The magnitude of this impact pressure increases significantly with wave height, as seen through the intensified red bands at the impact zone in Figures 3–5.

These localized impulses are consistent with theoretical predictions based on conservation of momentum and the Froude number, and they present key design concerns. Structures experiencing such steep gradient pressures must be reinforced at the base to prevent cracking, anchorage failure, or shear-induced movement. The ISPH–LES model accurately simulates the formation of these concentrated pressure zones, validating its applicability for assessing short-duration, high-magnitude loading.

In Cases 4 and 5, where the water depth behind the structure is increased, pressure is not only higher but also covers a wider region along the vertical face. This suggests the influence of higher hydrostatic backpressure and elevated energy levels in the impinging wave. The simulation reveals that overtopping behavior becomes more diffused, initiating earlier in the overtopping timeline, and the pressure is transmitted higher on the wall.

### Wave Crest Impact and Maximum Pressure Phase

The middle stages of the simulations correspond to the wave crest reaching the crest of the dam or wall. Here, in almost all cases, a sharp rise in pressure is observed both on the crest and downstream face - particularly in Cases 1, 5, and 8, which feature high wave energy and deeper

reservoirs. This phase simulates the maximum pressure exerted on the structure and is crucial for the assessment of surface damage, local scouring, and structural fatigue.

One key insight across all cases is the directional shift of pressure vectors - from vertical (during impact) to horizontal and downward (during overtopping). In this phase, the ISPH–LES model demonstrates strong agreement with physical expectations and experimental data in Kobel et al. [18], effectively capturing the complex, multiphase flow behavior of the wave as it wraps over the structure.

For Cases 6 and 7 - featuring sloped wall geometries - the model reveals a significantly lower peak pressure compared to vertical cases. The sloped face acts as a passive energy dissipation element, elongating the impact period and reducing peak values. This demonstrates the energy-reducing effect of inclined geometries and validates their role in modern coastal engineering practice. Similarly, in Cases 8 and 9, the broader crest widths result in a redistribution of pressure toward the rear crest edge, reducing localized loads on any single point.

These outcomes highlight the ISPH model's ability to capture small but critical shifts in pressure location and magnitude due to geometric modification, an important tool for engineers seeking optimized wave energy management in design.

## Dissipation and Post-Overtopping Phase

The final time frames illustrate the wave's energy dissipation phase. In most cases, pressure gradually subsides and reverts toward the base, accompanied by partial recirculation or backflow. Cases 1 to 3, involving lower reservoir depths, show relatively quick pressure drop-offs, indicating short-duration impulses and lower long-term structural stress. In contrast, Cases 4 and 5 demonstrate longer pressure tails - especially downstream - reflecting the prolonged presence of overtopping flow.

A critical observation is that in geometries with greater slope and width (Cases 6–9), pressure decay is both smoother and more gradual. This indicates a more favorable energy dissipation profile, less risk of structural resonance, and lower potential for erosive damage on downstream slopes. The simulation successfully visualizes pressure shedding and redistribution patterns, capturing not only the peak loads but the transient response of the structure to the wave's passage.

These findings are instrumental in identifying zones of prolonged exposure and informing choices related to downstream slope material (e.g., use of rock armor vs. concrete apron).

## Engineering Interpretation and Model Utility

The pressure results validate the ISPH–LES model's robustness in accurately reproducing complex wave-structure interactions. Key takeaways from this analysis include:

- Vertical walls experience sharper but more intense pressures—necessitating stronger reinforcement at the impact zone.
- Sloped geometries reduce peak pressures but increase the area of influence—useful for energy spread but requiring larger protected surfaces.
- Broader crest widths redistribute pressure over a larger footprint—beneficial for structural wear reduction.
- Pressure decay rates correlate well with wave volume and reservoir depth, confirming the physical accuracy of the model.

This level of analysis shows that the ISPH–LES framework can be confidently used for parametric studies, design optimization, and resilience assessment of coastal and hydraulic infrastructure subjected to impulsive wave conditions.

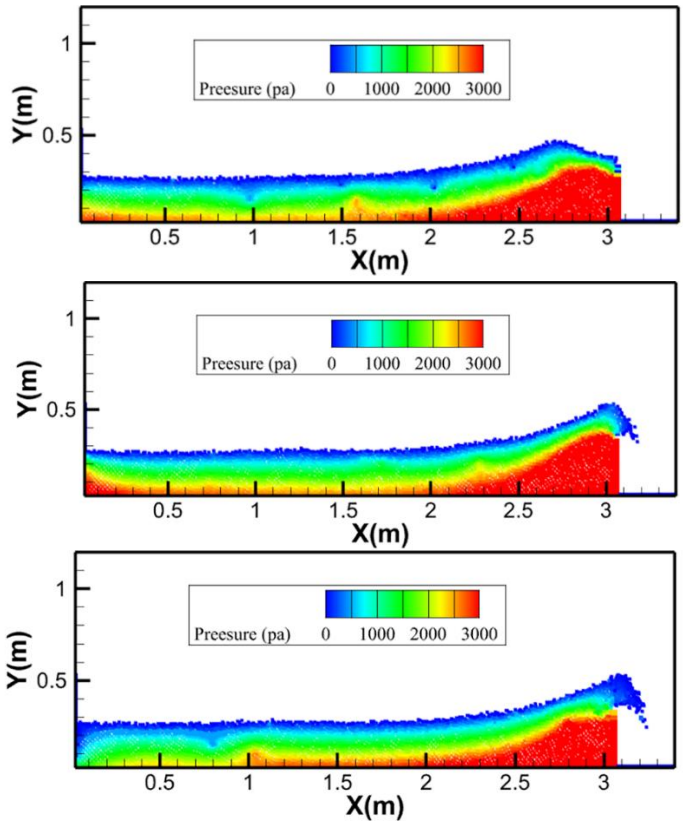



**Figure 3. Time Frame Pressure Distributions for Solitary Wave Overtopping: Case [1]**

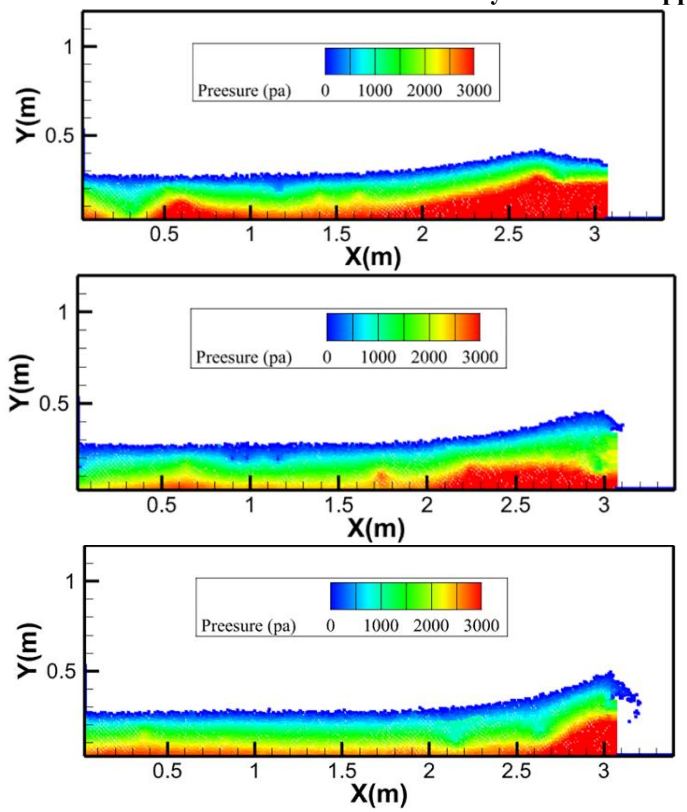



**Figure 4. Time Frame Pressure Distributions for Solitary Wave Overtopping: Case [2].**

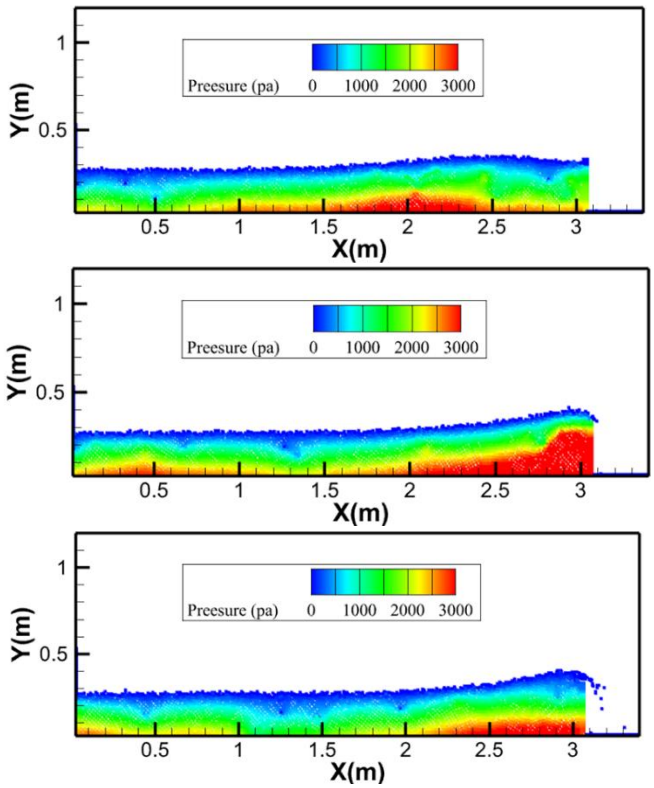



**Figure 5. Time Frame Pressure Distributions for Solitary Wave Overtopping: Case [3].**

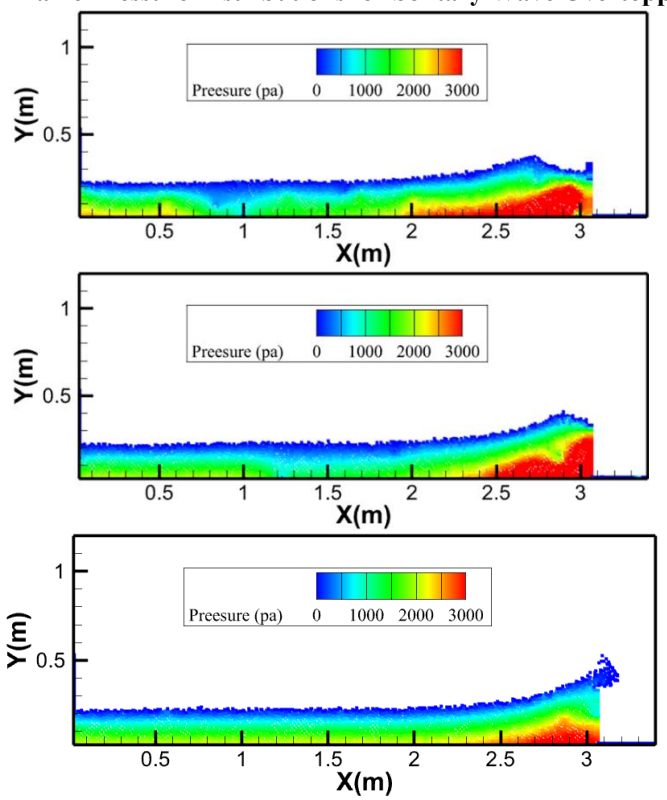



**Figure 6. Time Frame Pressure Distributions for Solitary Wave Overtopping: Case [4].**

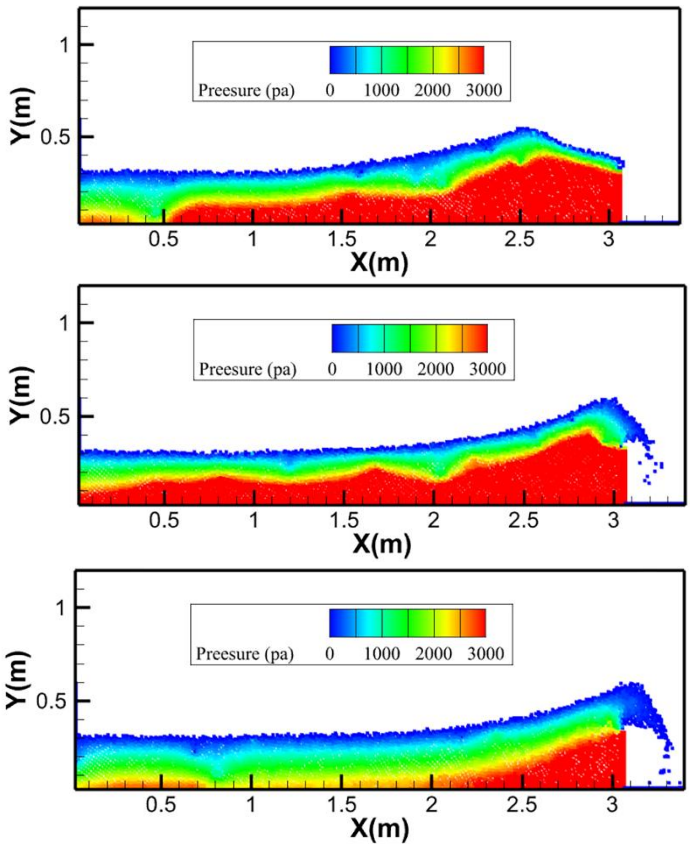



**Figure 7. Time Frame Pressure Distributions for Solitary Wave Overtopping: Case [5].**

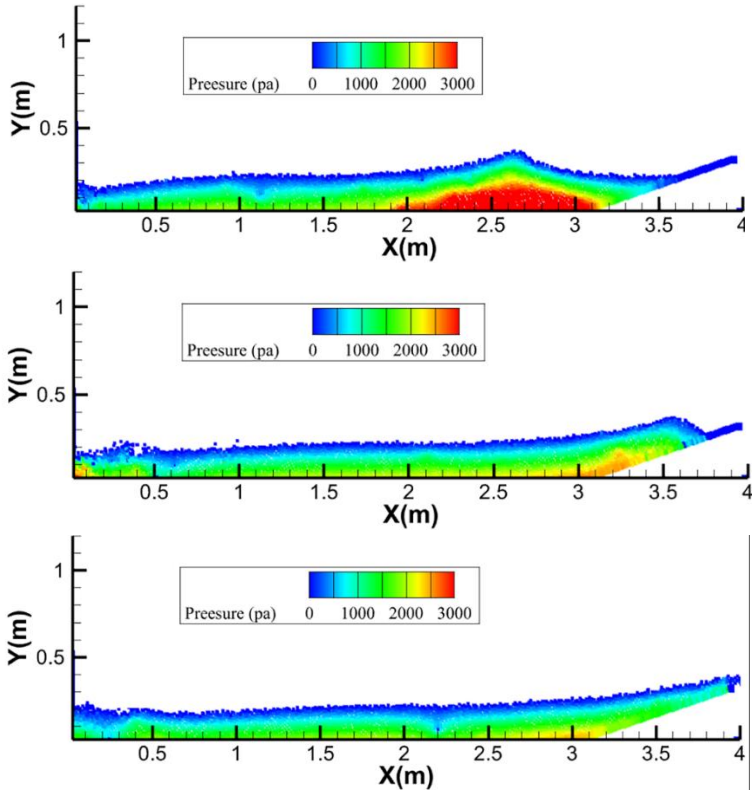



**Figure 8. Time Frame Pressure Distributions for Solitary Wave Overtopping: Case [6].**

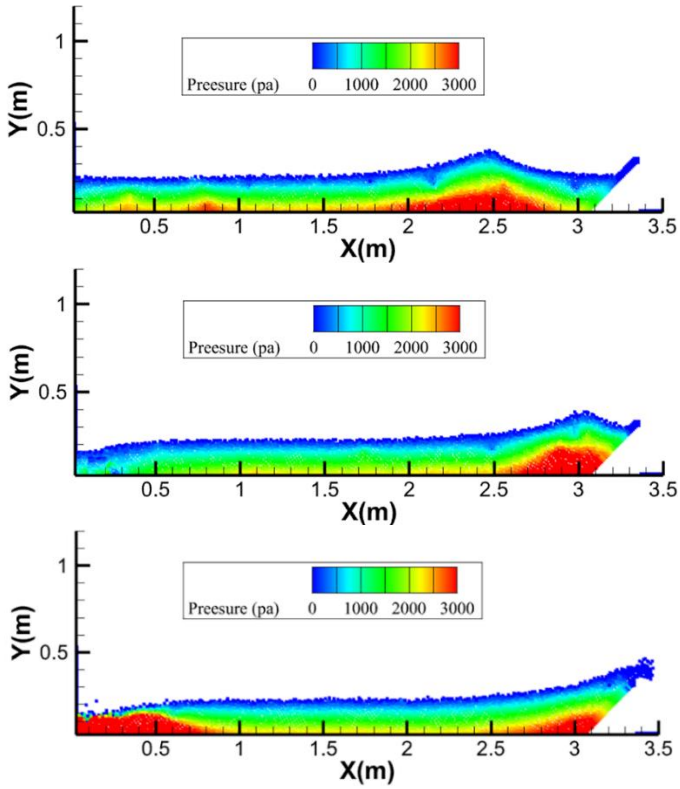



**Figure 9. Time Frame Pressure Distributions for Solitary Wave Overtopping: Case [7].**

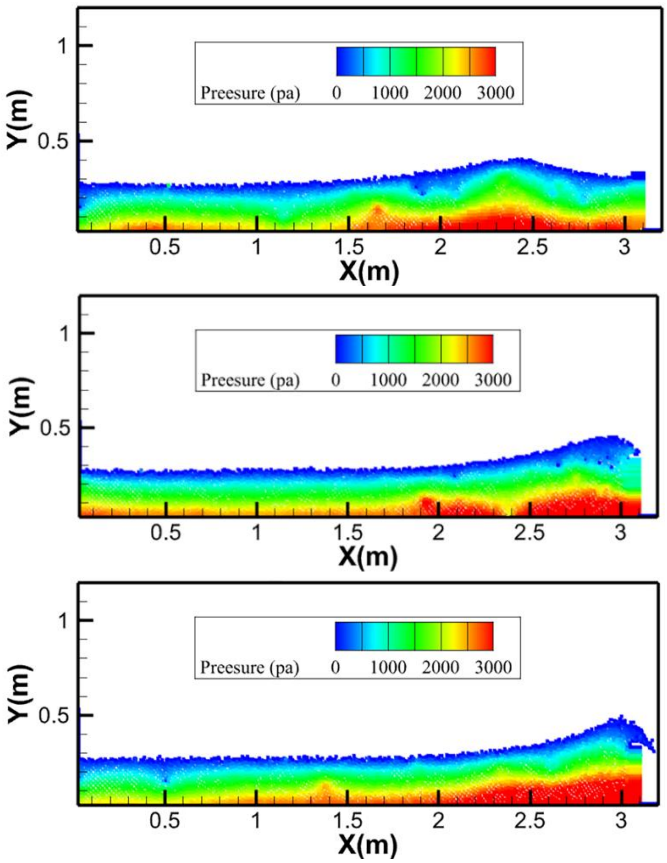



**Figure 10. Time Frame Pressure Distributions for Solitary Wave Overtopping: Case [8].**

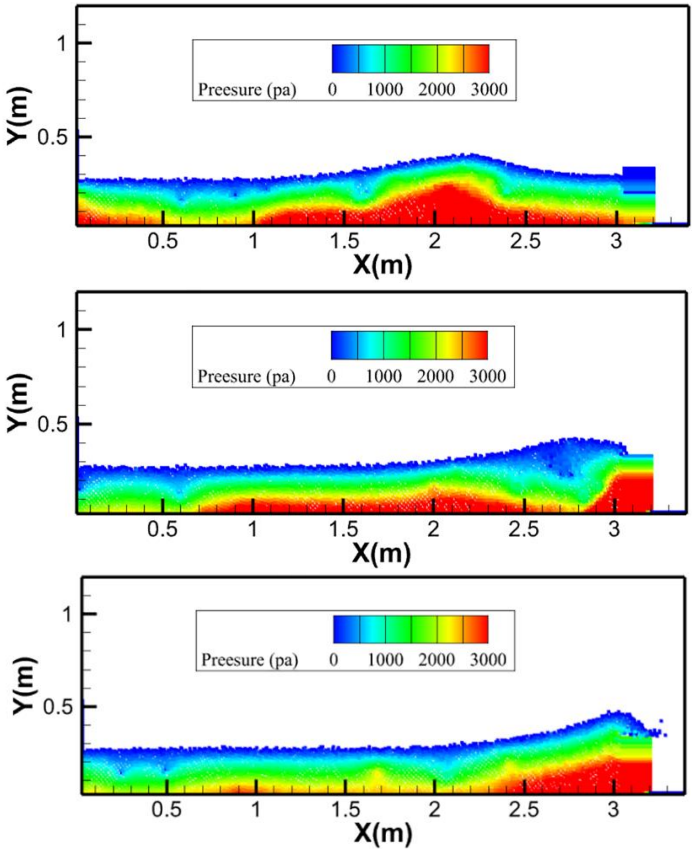



**Figure 11. Time Frame Pressure Distributions for Solitary Wave Overtopping: Case [9].**

## 4. Conclusion

This study presented a comprehensive numerical investigation of solitary wave overtopping at rigid hydraulic structures using a modified ISPH–LES (Incompressible Smoothed Particle Hydrodynamics – Large Eddy Simulation) model. The model was validated against experimental data across nine scenarios and demonstrated strong predictive accuracy with average errors of 9.5% for maximum overtopping depth, 15% for overtopping volume, and 5.9% for overtopping duration.

A key contribution of the study was the detailed analysis of temporal and spatial pressure distributions over 27-time frames per case. The model successfully captured the pressure build-up at impact, maximum crest pressures during overtopping, and dissipation patterns, all of which are critical for assessing structural integrity. It also reflected the effects of dam geometry variations (slope and crest width) on pressure magnitude and distribution, showing that sloped and wider geometries reduce localized peak pressures and help distribute wave energy more evenly.

The findings indicate that the ISPH–LES framework is highly reliable for simulating high-energy, turbulent overtopping flows and provides actionable engineering insights, such as identifying critical impact zones, supporting structural optimization, and improving protective design strategies. While the model showed robust performance under extreme overtopping conditions, further refinement is recommended for scenarios involving low-energy or short-duration overtopping events, where particle resolution and pressure diffusion may impact accuracy.

Overall, the ISPH–LES model proves to be a practical and high-fidelity tool for engineers and researchers engaged in the design, risk assessment, and resilience evaluation of coastal and hydraulic

infrastructures. Future work may extend this model's application to 3D configurations, real-time simulation scenarios, and integration with sediment transport or debris flow modules.

**Funding**

This research received no external funding.

**Conflict of interests**

The author declares that he has no conflict of interest.

**Artificial intelligence (AI) usage**

During the preparation of this work the author did not use any AI tools.

**Author Contributions**

All sections of the manuscript were prepared by the author.

## References

1. Kheybar H, Sajjadi SM, Ahadiyan J, Ghomeshi M. Hydraulic Analysis of Pivot Side Weirs with Sill. Iranian Journal of Soil and Water Research. 2025 Mar 21;56(1):229-46. https://doi.org/10.22059/ijswr.2024.382426.669790
2. Tahmasbipour M, Azizi Nadian H, Ahadiyan J, Oliveto G, Sajjadi SM, Kiyani AM. Experimental Investigation of T-Jump Stabilization Using Water Jets and Sinusoidal Corrugated Beds. Water. 2024 Dec 6;16(23):3513. https://doi.org/10.3390/w16233513
3. Taheri Talavari T, Sajjadi SM, Ahadiyan J, Azizi Nadian H. Numerical hydraulic and hydrodynamic investigation of flow passing through multiple elliptic lopac gates with Flow 3D software. Advanced Technologies in Water Efficiency. 2024 Sep 22;4(3):40-60. https://doi.org/10.22126/atwe.2024.10747.1127
4. Ahadiyan J, Chenari SA, Nadian HA, Katopodis C, Valipour M, Sajjadi SM, Omidvarinia M. Sustainable systems engineering by CFD modeling of lateral intake flow with flexible gate operations to improve efficient water supply. International Journal of Sediment Research. 2024 Aug 1;39(4):629-42. https://doi.org/10.1016/j.ijsrc.2024.05.003
5. Shahabi M, Ahadiyan J, Ghomeshi M, Narimousa M, Katopodis C, Azizi Nadian H. Numerical study of the effect of a V-shaped weir on turbulence characteristics and velocity in V-weir fishways. River Research and Applications. 2023 Jan;39(1):21-34. https://doi.org/10.1002/rra.4064
6. Sharoonizadeh S, Ahadiyan J, Scorzini AR, Di Bacco M, Sajjadi M, Moghadam MF. Turbulence characteristics of the flow resulting from the hydrodynamic interaction of multiple counter flow jets in expanding channels. Acta Mechanica. 2022 Sep;233(9):3867-80. https://doi.org/10.1007/s00707-022-03250-2
7. Mobarak F, Sajjadi SM, Ahadiyan J, Zeynivand M. Numerical modeling of the effect of elliptical elongation on the hydraulic performance of an elliptical Lopac gate. Water and Irrigation Management. 2022 Jun 22;12(2):263-75. https://doi.org/10.22059/jwim.2022.335817.952
8. Kheybar H, Sajjadi SM, Ahadiyan J. Effect of sudden canal contraction on the discharge coefficient and the energy dissipation coefficient of the elliptical LOPAC gate. Irrigation and Drainage. 2021 Dec;70(5):1145-54. https://doi.org/10.1002/ird.2622
9. Sarkamaryan S, Ahadiyan, J. Mathematical modeling of energy loss on Stepped Spillway Using ANSYS-CFX Numerical Model. Irrigation Sciences and Engineering. 2021 Mar;43(1):43-56. https://doi.org/10.22055/jise.2017.22269.1593
10. Noruzi S, Ahadiyan J. Effect of vortex breaker blades 45 degree on discharge coefficient of morning glory spillway using flow-3D. Journal of Irrigation

Sciences and Engineering. 2017 Jan 1;40(1):191-200. https://doi.org/10.22055/jise.2017.12677
11. EurOtop. Wave overtopping of sea defences and related structures: assessment manual. 2007. Available from: http://www.overtopping-manual.com/assets/downloads/EAK K073_EurOtop_2007.pdf
12. Özhan E, Yalcmer AC. Overtopping of solitary waves at model sea dikes. InCoastal Engineering 1990 1991 (pp. 1487-1498). https://doi.org/10.1061/9780872627765.113
13. Müller DR. Auflaufen und Überschwappen von Impulswellen an Talsperren (Doctoral dissertation, ETH Zurich).
14. Jervis M, Peregrine DH. Overtopping of waves at a wall: A theoretical approach. InCoastal Engineering 1996 1997 (pp. 2192-2205). https://doi.org/10.1061/9780784402429.170
15. Stansby PK. Solitary wave run up and overtopping by a semi-implicit finite-volume shallow-water Boussinesq model. Journal of Hydraulic Research. 2003 Nov 1;41(6):639-47. https://doi.org/10.1080/00221680309506896
16. Xiao H, Huang W, Tao J. Numerical modeling of wave overtopping a levee during Hurricane Katrina. Computers & Fluids. 2009 May 1;38(5):991-6. https://doi.org/10.1016/j.compfluid.2008.01.025
17. Heller V, Hager WH, Minor HE. Landslide generated impulse waves in reservoirs: Basics and computation. VAW-Mitteilungen. 2009;211. https://doi.org/10.1142/9789814277426_0109
18. Kobel J, Evers FM, Hager WH. Impulse wave overtopping at rigid dam structures. Journal of Hydraulic Engineering. 2017 Jun 1;143(6):04017002. https://doi.org/10.1061/(asce)hy.1943-7900.0001271
19. Chi SH, Zhang C, Sui TT, Cao ZB, Zheng JH, Fan JS. Field observation of wave overtopping at sea dike using shore-based video images. Journal of Hydrodynamics. 2021 Aug;33(4):657-72. https://doi.org/10.1007/s42241-021-0073-1
20. Hirt CW, Nichols BD. Volume of fluid (VOF) method for the dynamics of free boundaries. Journal of computational physics. 1981 Jan 1;39(1):201-25. https://doi.org/10.1016/0021-9991(81)90145-5
21. Monaghan JJ. Simulating free surface flows with SPH. Journal of computational physics. 1994 Feb 1;110(2):399-406. https://doi.org/10.1006/jcph.1994.1034
22. Van der Meer JW, Petit HA, Van den Bosch P, Klopman G, Broekens RD. Numerical simulation of wave motion on and in coastal structures. InCoastal Engineering 1992 1993 (pp. 1772-1784). https://doi.org/10.1061/9780872629332.134
23. Memarzadeh R, Barani G, Ghaeini-Hessaroeyeh M. Numerical modeling of sediment transport based on unsteady and steady flows by incompressible smoothed particle hydrodynamics method. Journal of Hydrodynamics. 2018 Oct; 30:928-42. https://doi.org/10.1007/s42241-018-0111-9
24. Memarzadeh R, Barani G, Ghaeini-Hessaroeyeh M. Application of a weakly compressible smoothed particle hydrodynamics multi-phase model to non-cohesive embankment breaching due to flow overtopping. Frontiers of Structural and Civil Engineering. 2018 Sep; 12:412-24. https://doi.org/10.1007/s11709-017-0432-8
25. Dalrymple RA, Rogers BD. Numerical modeling of water waves with the SPH method. Coastal engineering. 2006 Feb 1;53(2-3):141-7.

https://doi.org/10.1016/j.coastaleng.2005.10.004
26. Memarzadeh R, Hejazi K. ISPH numerical modeling of nonlinear wave run-up on steep slopes. J Persian Gulf (Marine Sci). 2012;10(3):17–26.
27. Lind SJ, Xu R, Stansby PK, Rogers BD. Incompressible smoothed particle hydrodynamics for free-surface flows: A generalised diffusion-based algorithm for stability and validations for impulsive flows and propagating waves. Journal of Computational Physics. 2012 Feb 20;231(4):1499-523. https://doi.org/10.1016/j.jcp.2011.10.027
28. Didier E, Neves DR, Martins R, Neves MG. Wave interaction with a vertical wall: SPH numerical and experimental modeling. Ocean engineering. 2014 Sep 15; 88:330-41. https://doi.org/10.1016/j.oceaneng.2014.06.029
29. He M, Gao XF, Xu WH. Numerical simulation of wave-current interaction using the SPH method. Journal of Hydrodynamics. 2018 Jun;30(3):535-8. https://doi.org/10.1007/s42241-018-0042-5
30. Tsurudome C, Liang D, Shimizu Y, Khayyer A, Gotoh H. Incompressible SPH simulation of solitary wave propagation on permeable beaches. Journal of Hydrodynamics. 2020 Aug; 32:664-71. https://doi.org/10.1007/s42241-020-0042-0
31. Wang Z, Zhang C, Haidn OJ, Hu X. An Eulerian SPH method with WENO reconstruction for compressible and incompressible flows. Journal of Hydrodynamics. 2023 Apr;35(2):210-21. https://doi.org/10.1007/s42241-023-0025-z
32. Feng R, Fourtakas G, Rogers BD, Lombardi D. Modelling internal erosion using 2D smoothed particle hydrodynamics (SPH). Journal of Hydrology. 2024 Aug 1; 639:131558. https://doi.org/10.1016/j.jhydrol.2024.131558
33. Akbari H. Simulation of wave overtopping using an improved SPH method. Coastal Engineering. 2017 Aug 1; 126:51-68. https://doi.org/10.1016/j.coastaleng.2017.04.010
34. Luo M, Reeve DE, Shao S, Karunarathna H, Lin P, Cai H. Consistent Particle Method simulation of solitary wave impinging on and overtopping a seawall. Engineering Analysis with Boundary Elements. 2019 Jun 1; 103:160-71. https://doi.org/10.1016/j.enganabound.2019.03.012
35. Aly AM, Asai M, Sonda Y. Modelling of surface tension force for free surface flows in ISPH method. International Journal of Numerical Methods for Heat & Fluid Flow. 2013 Apr 12;23(3):479-98.
36. Shao S, Lo EY. Incompressible SPH method for simulating Newtonian and non-Newtonian flows with a free surface. Advances in water resources. 2003 Jul 1;26(7):787-800. https://doi.org/10.1016/s0309-1708(03)00030-7
37. Shao S. Incompressible smoothed particle hydrodynamics simulation of multifluid flows. International Journal for Numerical Methods in Fluids. 2012 Aug 20;69(11):1715-35. https://doi.org/10.1002/fld.2660
38. Lee JJ, Skjelbreia JE, Raichlen F. Measurement of velocities in solitary waves. Journal of the Waterway, Port, Coastal and Ocean Division. 1982 May;108(2):200-18. https://doi.org/10.1061/jwpcdx.00002

© 2025 by the authors. Licensee SCU, Ahvaz, Iran. This article is an open access article distributed under the terms and conditions of the Creative Commons Attribution 4.0 International (CC BY 4.0 license) (http://creativecommons.org/licenses/by/4.0/).